View metadata, citation and similar papers at core.ac.uk
brought to you by CORE
provided by Online Research Database In Technology

Technical University of Denmark

Oxidation and Reduction of Liquid SnPb (60/40) under Ambient and Vacuum Conditions

Kuhmann, Jochen Friedrich; Maly, K.; Preuss, A.; Adolphi, B.; Wirth, T.; Oesterle, W.; Fanciulli, M.; Weyer, G.

Published in:
Electrochemical Society. Journal

Link to article, DOI:
10.1149/1.1838608

Publication date:
1998

Document Version
Publisher's PDF, also known as Version of record

Link back to DTU Orbit

Citation (APA):
Kuhmann, J. F., Maly, K., Preuss, A., Adolphi, B., Wirth, T., Oesterle, W., ... Weyer, G. (1998). Oxidation and Reduction of Liquid SnPb (60/40) under Ambient and Vacuum Conditions. Electrochemical Society. Journal, 145(6), 2138-2142. DOI: 10.1149/1.1838608

DTU Library
Technical Information Center of Denmark

General rights
Copyright and moral rights for the publications made accessible in the public portal are retained by the authors and/or other copyright owners and it is a condition of accessing publications that users recognise and abide by the legal requirements associated with these rights.

- Users may download and print one copy of any publication from the public portal for the purpose of private study or research.
- You may not further distribute the material or use it for any profit-making activity or commercial gain
- You may freely distribute the URL identifying the publication in the public portal

If you believe that this document breaches copyright please contact us providing details, and we will remove access to the work immediately and investigate your claim.

Oxidation and Reduction of Liquid SnPb (60/40) under Ambient and Vacuum Conditions

J. F. Kuhmann,[a] K. Maly,[b] A. Preuβ,[c] B. Adolphi,[c] K. Drescher,*[,c] T. Wirth,[d] W. Oesterle,[d] M. Fanciulli,[e] and G. Weyer[e]

[a]*Mikroelektronik Centret, Denmark Technical University, DK-2400 Lyngby, Denmark*
[b]*Heinrich-Hertz-Institut Berlin, Germany*
[c]*Institut für Halbleiter und Mikrosystemtechnik, Technische Universität Dierden Dresden, Germany,*
[d]*Bundesanstalt für Materialforschung, Berlin, Germany*
[e]*University of Aarhus, Denmark*

ABSTRACT

One of the most straightforward approaches to fluxless solder bonding is using vacuum conditions to prevent further oxidation and, where needed, to reduce solder oxides by the use of molecular hydrogen (H_2).[1-3] This study on oxidation and reduction of solder oxides on SnPb (60/40) is aimed to provide a better understanding for fluxless solder bonding applications under controlled atmospheric conditions. By means of scanning Auger spectroscopy it is shown, that growth of oxide films on metallic SnPb above the eutectic temperature can be significantly reduced by decreasing the O_2 partial pressure up to $\sim 10^{-5}$ Pa. The native oxide, which was left on top of one part of the samples, prevented a further scale growth even during heating at temperatures above the melting point. The native oxide consists of SnO_2, which has most likely an amorphous structure, whereas the oxide, grown at 200 and 250°C is crystalline SnO. For sample preparation, the reduction of the native oxide on eutectic SnPb was carried out successfully using low temperature (250°C) and short heating cycles (2 min). The effectiveness of H_2 to reduce SnO_2 at typical soldering parameters (240°C, < 2 min) was furthermore proven by in situ Auger electron spectroscopy.

Introduction

Oxide on solder surfaces leads to poor wetting and bad adhesion of the assembled parts. In general, fluxes are used to take away the oxides and surface contaminations and protect the solder from reoxidation.

For the assembly of photonic devices and micromachined systems, however, fluxes should be avoided. In photonics fluxes can degrade the unprotected devices or attenuate the optical signal. In the case of micromechanical devices, fluxes can clog nozzles and orifices or destroy sensitive membranes. In microelectronics, fluxless soldering is under investigation for economic reasons and for reliability improvements.

The starting point for soldering operations is a solder surface covered by its native oxide. The native oxide on SnPb (60/40) has a thickness of ~3 nm, which remains unaffected even after extended shelf storage of 3 months; even after 1 year, the oxide will only insignificantly grow.[4]

The oxide growth on SnPb (60/40) at temperatures below 120°C follows a logarithmic law, whereas at higher temperatures, parabolic growth kinetics can be observed.[5,6] At temperatures of 160 and 170°C, an increase in thickness of up to approximately 20 nm after 80 days has been reported.[7] The oxide layers on SnPb (60/40) were found to contain both tin and lead, with tin being oxidized preferentially.

The oxide on solid and liquid tin was reported to consist of both stannous oxide and stannic oxide (SnO and SnO_2).[8,9] Britton et al.[10,11] examined oxide films grown on Sn at temperatures below 180°C using transmission electron microscopy (TEM). The authors did not observe any electron diffraction pattern whereas Boggs[12] identified the oxide, grown on Sn at 75°C as crystalline α-SnO. The author pointed out that the samples needed to be heated long enough (>800 h) to obtain enough crystalline material.

The oxidation of liquid SnPb (60/40) at different temperatures has been investigated by different authors.[13-15] All oxidations were carried out under ambient, the starting point of oxidation being fresh, metallic solder surfaces. In all experiments, a parabolic growth of the oxide layers has been observed, the actual thickness depending very much on the sample preparation and the employed analysis technique (Fig. 1). Electron diffraction of the oxidized samples identified SnO and SnO, and also PbO.

In addition to that, a considerable amount of publications exist that focus on surface tension measurements of Sn and the influence of oxidation on the surface tension. In Ref. 16, a kinetic and fluodynamic model is described which gives, in addition to thermodynamic models, the influence of gas flow parameters and geometry on the oxidation of Sn. The model nevertheless excludes high vacuum conditions employed in this study. The influence of oxidation on surface tension has been investigated in Ref. 17. Here, a distinct drop in surface tension at temperatures between 300 and 500°C was observed by increasing the O_2 partial pressure from 10^{-16} to 10^{-6} Pa. To obtain these pressures the authors used a helium/hydrogen mixture. Data obtained in high vacuum (5×10^{-6} to 1×10^{-7} Pa) showed especially in the range of 250 to 400°C extensive scattering. Another investigation on surface tension of Sn[18] found that at an O_2 partial pressure of 4×10^{-6} Pa at 290°C, no oxygen peak was detected during Auger electron spectroscopy (AES) on the surface of the molten Sn droplet for 2 h.

SnO_2 is the thermodynamically most stable oxide below 250°C

$$Sn + O_2 \rightleftarrows SnO_2 \quad [1]$$

$$p_{O_2}\,(250°C) = 10^{-43}\ \text{Pa} \quad [2]$$

Equation 1 describes the oxidation of Sn to stannic oxide (SnO_2). For equilibrium conditions ($\Delta G = 0$), the reaction

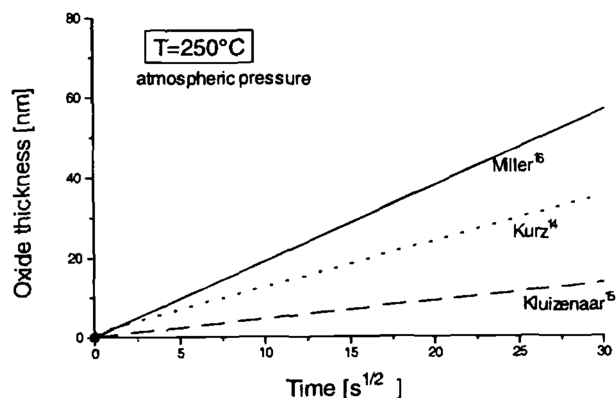

Fig. 1. Fitted data of parabolic oxide growth on SnPb (60/40) at 250°C in ambient.

* Electrochemical Society Active Member.

Downloaded 28 Jun 2010 to 192.38.67.112. Redistribution subject to ECS license or copyright; see http://www.ecsdl.org/terms_use.jsp

Table I. Thermochemical data on Sn and Pb oxides and on H_2/H_2O ratios which determine the O_2 equilibrium partial pressures for the oxidation at a given temperature.[24]

T (°C)	G^0 (J/mol 10^5)				p_{O_2GG} (Pa)				p_{H_2}/p_{H_2O}			
	SnO	SnO_2	PbO	PbO_2	SnO	SnO_2	PbO	PbO_2	SnO	SnO_2	PbO	PbO_2
150	−4.90	−4.93	−3.54	−2	$2 \cdot 10^{-56}$	$1 \cdot 10^{-56}$	$2 \cdot 10^{-39}$	$2 \cdot 10^{-20}$	590	840	$2 \cdot 10^{-6}$	$7 \cdot 10^{-16}$
200	−4.82	−4.83	−3.44	−1.91	$7 \cdot 10^{-49}$	$4 \cdot 10^{-49}$	$1 \cdot 10^{-33}$	$8 \cdot 10^{-17}$	170	210	$5 \cdot 10^{-6}$	$1 \cdot 10^{-14}$
250	−4.74	−4.74	−3.34	−1.81	$4 \cdot 10^{-43}$	$4 \cdot 10^{-43}$	$2 \cdot 10^{-28}$	$8 \cdot 10^{-14}$	82	80	$8 \cdot 10^{-6}$	$2 \cdot 10^{-13}$
300	−4.64	−4.63	−3.24	−1.72	$4 \cdot 10^{-38}$	$5 \cdot 10^{-38}$	$4 \cdot 10^{-24}$	$2 \cdot 10^{-11}$	35	31	$1 \cdot 10^{-5}$	$1 \cdot 10^{-12}$
350[a]	−4.54	−4.52	−3.14		$7 \cdot 10^{-34}$	$1 \cdot 10^{-33}$	$2 \cdot 10^{-21}$		16	13	$2 \cdot 10^{-5}$	

[a] For PbO_2 data only, available for temperatures up to 314°C.

is determined by the change in the Gibbs free energy ΔG^0 at a given temperature, and the O_2 partial pressure, p_{O_2}, normalized by the O_2 partial pressure under standard conditions, $p^0_{O_2}$, as described in Eq. 2. The values for ΔG^0 and for p_{O_2} can be taken from Table I. For values above p_{O_2}, oxidation of Sn will still occur. For values below p_{O_2}, which is, e.g., 10^{-43} Pa at 250°C, the oxide will decompose. In order to achieve values in that order of magnitude the reaction of H_2 with O_2

$$2H_2O + O_2 \rightleftarrows 2H_2O \quad [3]$$

$$p_{O_2} = \frac{p(H_2O)^2}{p(H_2)} \exp \frac{\Delta G^0}{RT} \quad [4]$$

can be utilized (Eq. 3). At a given temperature, this reaction determines the O_2 partial pressure according to Eq. 4. The values for this reaction which result in an O_2 partial pressure of 10^{-43} Pa are given in terms of the p_{H_2}/p_{H_2O} ratios in Table I.

H_2 has been successfully used in the surface tension studies on Sn which were mentioned above to obtain oxide free surfaces. Nevertheless, the effectiveness of H_2 to reduce Sn oxides at typical soldering temperatures is misconceived in some technical publications.[19-21]

This might partly be due to one study published in Ref. 22 on the reduction kinetics of some metal oxides. By means of differential thermal analysis (DTA), it was found that the decomposition of the stannic oxide powder under H_2 atmosphere only started above (400°C). For the reduc-

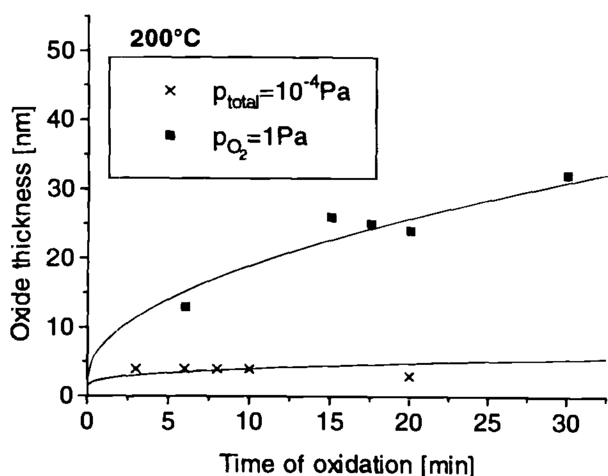

Fig. 2. Scale growth on liquid SnPb (60/40) at different pressures at 200°C.

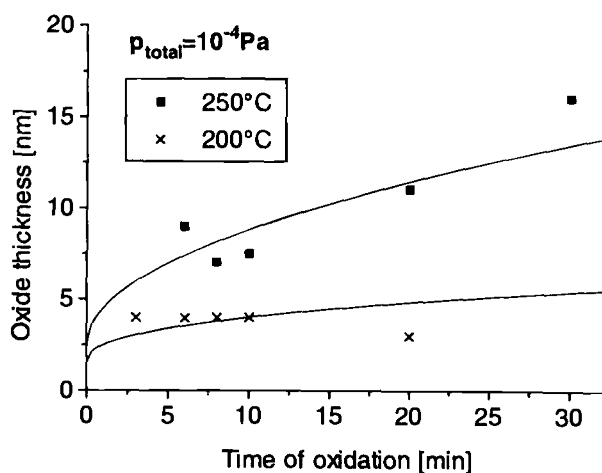

Fig. 4. Scale growth on liquid SnPb (60/40) at 10^{-4} Pa at 200 and 250°C.

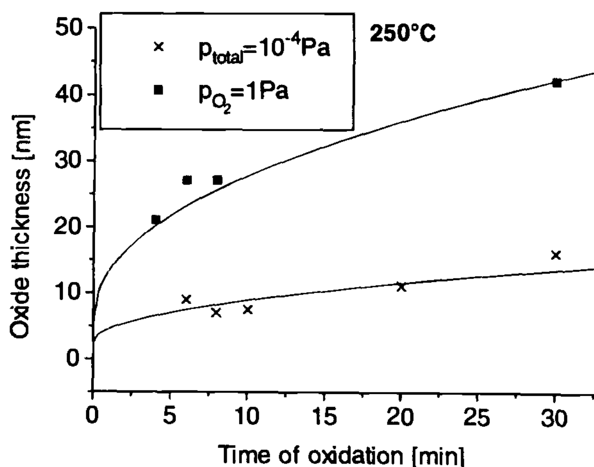

Fig. 3. Scale growth on liquid SnPb (60/40) at different pressures at 250°C.

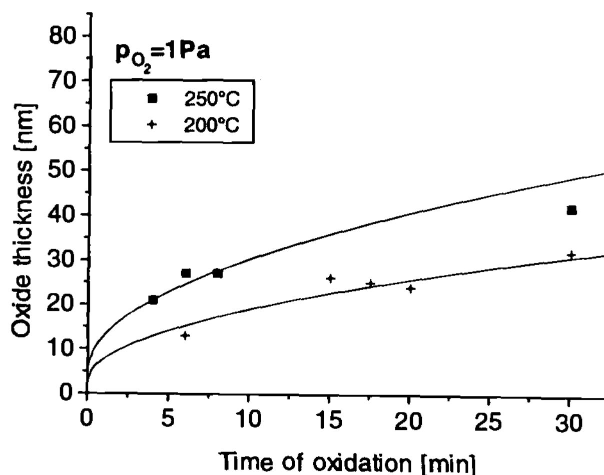

Fig. 5. Scale growth on liquid SnPb (60/40) at 1 Pa O_2 pressure at 200 and 250°C.

Downloaded 28 Jun 2010 to 192.38.67.112. Redistribution subject to ECS license or copyright; see http://www.ecsdl.org/terms_use.jsp

Table II. Sample preparation.

Starting point	Solder, covered by native oxide		Fresh solder[a]	
Temperature	200°C	250°C	200°C	250°C
Heating duration	min	min	min	min
Atmospheric pressure	5/10/20	6/10/15/20/30		
$p_{total.} = 10^{-4}$ Pa	3/5/10/20	6/10/15/20/30	3/6/8/10/20	6/8/10/20/30
$p_{O_2} = 1$ Pa			6/15/17, 5/20/30	4/6/8/10/20/30

[a] Fresh solder surfaces were obtained by reduction of the oxide with H_2 at 250°C for 2 min.

tion of PbO by H_2, the temperature needed was reported to be 319°C.

Experimental and Results

Oxidation kinetics.—The investigation of oxide growth on the heat-treated samples was carried out by scanning Auger measurement (SAM). The energies of the Ar^+ beam and electron beam were 1 and 3 keV, respectively. The diameter of the electron beam was 500 nm, the scanned area was approximately 100 × 100 μm. For the determination of sputter rates, SnO_2 and PbO layers of known thickness were sputtered. The average of the measured sputter rates (25 nm/min) was used to obtain the oxide thickness from sputter profiles. Sensitivity factors were experimentally determined to correct for sputter and matrix effects and to obtain the unbiased concentration values.

The SnPb (60/40) solder was coevaporated on metallized (Ti/Pt as adhesion and wetable metal, respectively) Si substrates using high purity materials. After evaporation, the samples were molten in an inert organic medium to homogenize. After that, the samples were cleaned and heat-treated under different levels of O_2 partial pressures. For the oxidation a vacuum chamber with glass plates on top and bottom was used. A focused IR radiation source was used to heat the samples. This configuration allowed rapid heating (≤30 K/s) and cooling rates, the samples being heated solely by absorption of light. This configuration also provided stable vacuum conditions during the heat-treatment, since heating of the chamber walls was avoided. The samples were treated at 200 and 250°C in ambient and under vacuum conditions. One part of the samples was treated with the native oxide layer as a starting point, in the rest of the samples, the native oxide layer was reduced by H_2 prior to the oxidation.

The native oxide was measured for samples having been stored 3 days and 3 months at *RT* in ambient. Regardless of storage duration for both oxide layers, a thickness of ~3 nm was measured. Figure 6 gives a surface spectrum of the

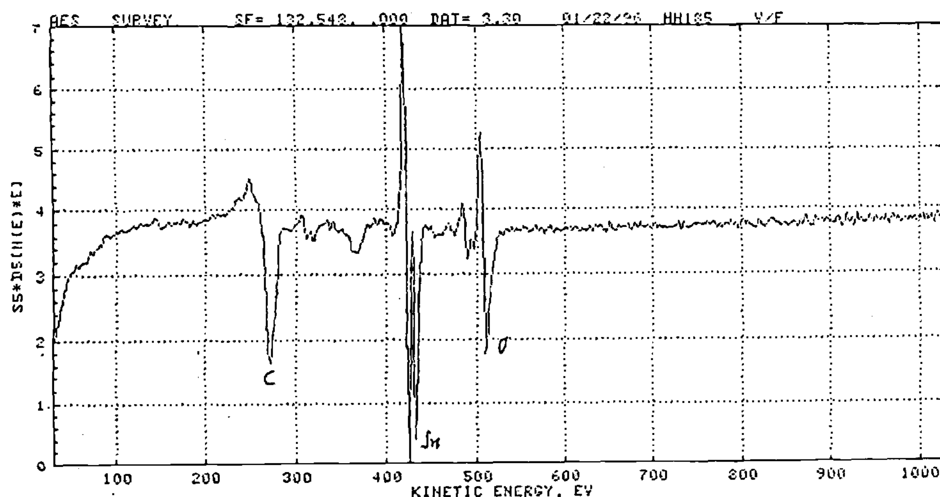

Fig. 6. AES spectrum before sputtering (survey).

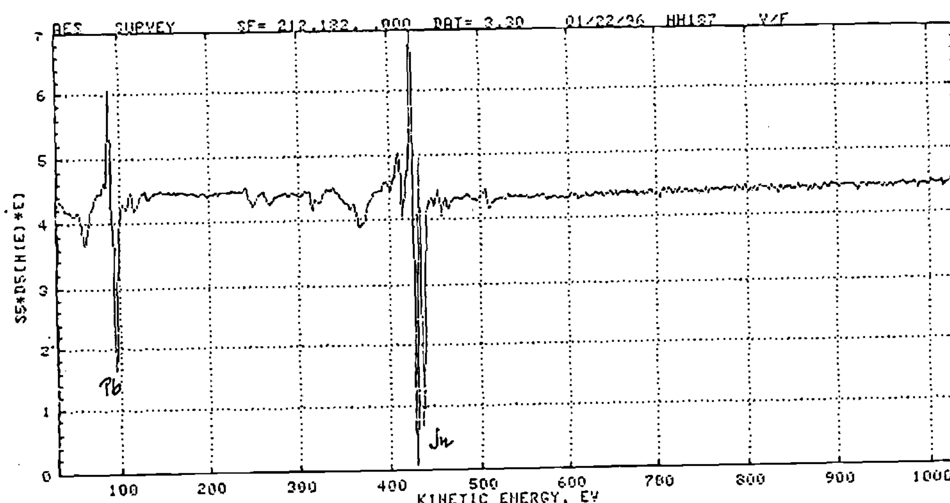

Fig. 7. AES spectrum after sputtering.

Downloaded 28 Jun 2010 to 192.38.67.112. Redistribution subject to ECS license or copyright; see http://www.ecsdl.org/terms_use.jsp

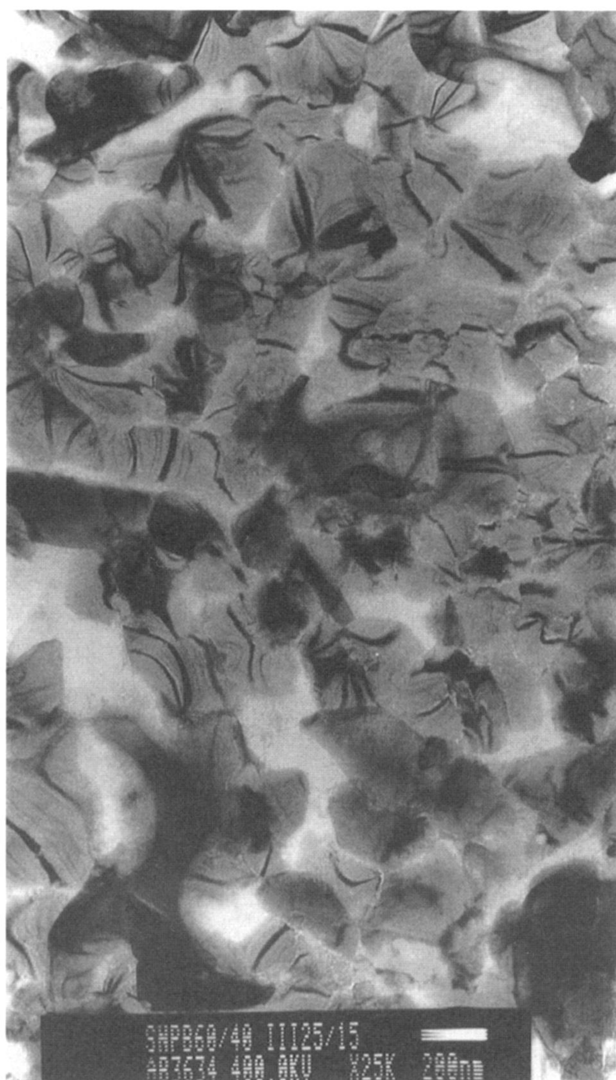

Fig. 8. TEM picture of SnO crystallites, formed on the metallic solder at 250°C.

native oxide layers: Besides typical surface contaminants like C and in some cases also small amounts of S and Cl the spectrum only consisted of Sn and O. Figure 7 shows the spectrum after the oxide has been sputtered. After characterization of the native oxide, the samples were heat-treated in different atmospheres according to Table II.

The samples with the native oxide as starting point of the oxidation exhibited, after treatment in high vacuum and even in ambient at temperatures of 200 and 250°C, no significant increase in oxide thickness. Only one sample, treated at 250°C in high vacuum ($p_{total} = 10^{-4}$ Pa) for 30 min, had an increased oxide thickness of 7 nm. Two samples treated in ambient at 250°C for 10 and 30 min exhibited a scale growth of 12 nm and even 50 nm thickness. This growth, however, was not confirmed by the rest of the samples, and thus was attributed to rupture of the oxide layers during heat-treatment.

The scale growth of the samples, which were reduced by H_2 (250°C, 2 min) prior to oxidation are given in Fig. 2-5. To guide the eye, the curves were fitted to a parabolic law. The growth of the scales could be significantly reduced in vacuum. Especially at the higher O_2 pressure (1 Pa) some samples showed erratic scale growth, which was, again, attributed to rupture of the growth-limiting oxide layer. To illustrate the dependence of oxidation on temperature, the values shown in Fig. 2 and 3 are replotted in Fig. 4 and 5 for $p_{total} = 10^{-4}$ Pa and $p_{O_2} = 1$ Pa.

Characterization of the oxide.—The native oxide and the oxide, grown on the molten, metallic solder surface, have been investigated by TEM. For this purpose, a thin carbon layer (~20 nm) was evaporated onto the samples to improve handling of the very thin oxide films. Then the oxide was extracted from the solder by a selective enchant. Figure 8 shows a TEM micrograph of polycrystalline oxide layer grown at 250°C which was identified by single area electron diffraction as consistent with the SnO-phase. Figure 9 gives the energy dispersive X-ray (EDX) spectrum of the analyzed area. The Cu in the spectrum stems from the Cu net, which was used to handle the extracted films.

Extractions of the native oxide layer did not yield in any diffraction pattern. Due to the thinness of the native oxide (3 nm), it proved impossible to characterize the samples with EDX. The samples were therefore characterized using Mössbauer spectroscopy (MS) (Fig. 10). The native oxide was found to consist of SnO_2.

Reduction.—Reduction experiments were carried out in situ, using modified AES equipment. Evaporated and homogenized SnPb (60/40) samples on Pt metallized substrates were introduced into the chamber and heated up to 240°C. The Pt was covered by the solder from the start and only served as a wetable metallization. Then H_2 was in-

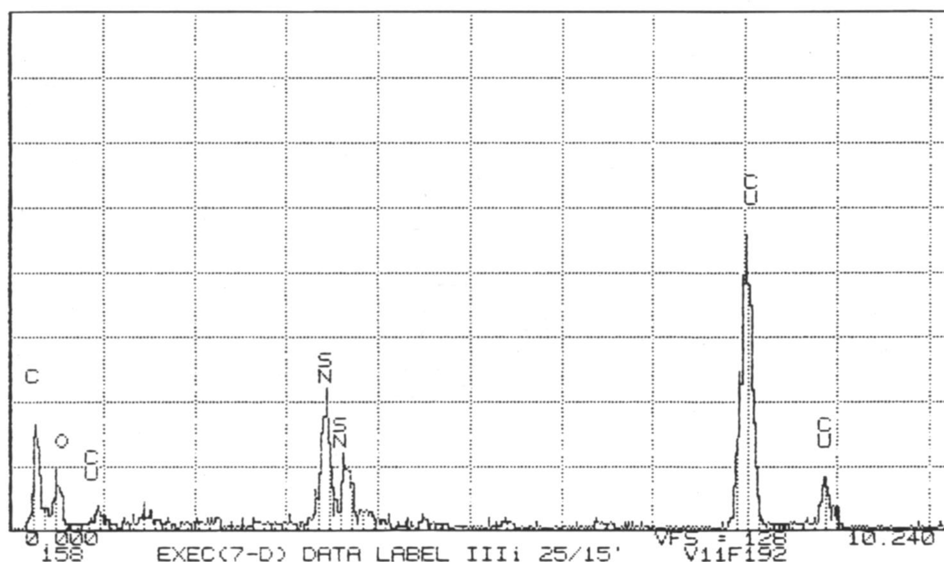

Fig. 9. EDX spectrum of the material, shown in Fig. 8.

Downloaded 28 Jun 2010 to 192.38.67.112. Redistribution subject to ECS license or copyright; see http://www.ecsdl.org/terms_use.jsp

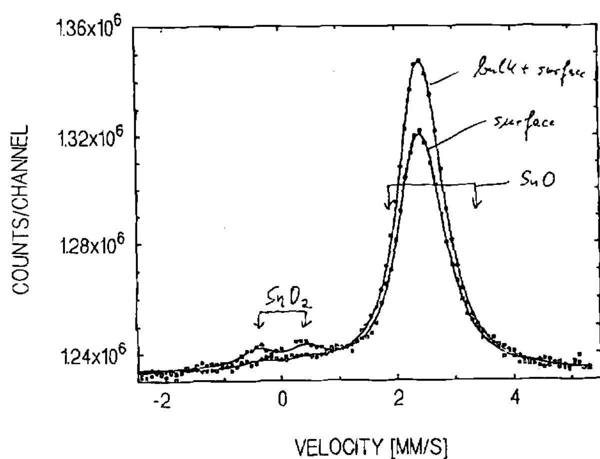

Fig. 10. Mössbauer spectroscopy of the native oxide; only SnO_2 could be detected.

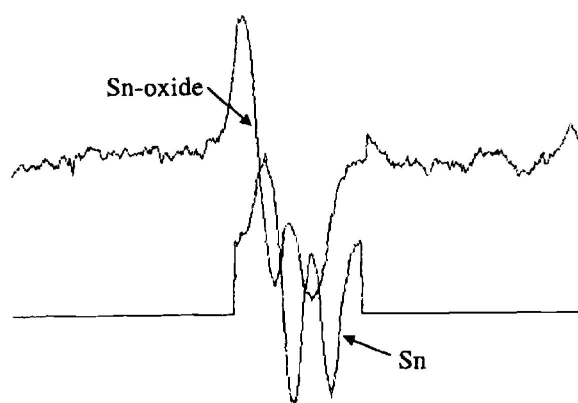

Fig. 11. Energy shift between Sn oxide and metallic tin, induced by H_2 treatment at 240°C for 2 min ($H_2/H_2O \geq 100$).

jected, leading to a rise of pressure from 10^{-9} to 10^{-7} Pa. To monitor the reduction the energy shift of the spectrum from oxidized to metallic tin was chosen.[18,23] The spectra shown in Fig. 11 were taken during one run. The Sn peak was measured around 430 eV. A scale in Fig. 11 is omitted, since the absolute values are dependent on experimental setup and not important if the aim of the measurement is to measure the difference of Sn in the oxidized and metallic state. Only a short time (<2 min) after the introduction of H_2, the characteristic energy shift of ~4 eV between the Sn oxide and metallic Sn could be observed (Fig. 11).

Conclusion

This study proves that applying vacuum or lowering the soldering temperatures to, e.g., 200°C, can significantly decrease the oxide growth on metallic SnPb (60/40).

The native oxide, which has been investigated by MS, consists of SnO_2. Electron diffraction of the native oxide films did not yield any patterns. An amorphous structure of the native oxide is most likely. This finding is also in agreement with the literature.[12] The different growth kinetics of the samples with and without the native oxide as a starting point can therefore be explained by different oxide morphologies; the short-circuit diffusion paths of a crystalline oxide lead to much faster oxide growth, and the samples, covered by the native, presumably amorphous oxide, are much better protected against further oxidation.

Using in situ AES it was demonstrated furthermore, that H_2 is able to reduce the oxide on SnPb solders at typical soldering temperatures (e.g., 240°C). The reduction was measured, using the characteristic energy shift of the Auger spectrum of oxidized and metallic tin of ~4 eV. Provided the necessary thermodynamic boundary are met conditions (Table I) the reduction of the SnO_2 takes place with no delay. This means, that H_2 can be effectively used for soldering applications, which do not allow the use of conventional fluxing agents.

Manuscript submitted June 17, 1997; revised manuscript submitted March 4, 1998.

Mikroelectronik Centret, Denmark Technical University, assisted in meeting the publication costs of this article.

REFERENCES

1. J. F. Kuhmann, H.-J. Hensel, and H.-G. Bach, in *Proceedings of the EuPac '96 Conference*, DVS, pp. 37-40, (1996).
2. J. F. Kuhmann, H.-J. Hensel, and H.-G. Bach, in *Proceedings of the 46th ECTC Conference*, CPMT IEEE, pp. 1088-1092 (1996).
3. J. F. Kuhmann and D. Pech, *IEEE Photonic Technol. Lett.*, **8** (1996).
4. *Metals Handbook*, 9th ed., Vol. 13, *Corrosion*, ASM International, Metals Park, OH (19xx).
5. R. A. Konetzki, Y. A. Chang, and V. C. Marcotte, *J. Mater. Res.*, **4**, 1421 (1989).
6. R. A. Konetzki, M. X. Zhang, D. A. Sluzewski, and Y. A. Chang, *J. Electron. Pack.*, **112**, 175 (1990).
7. G. Di Giacomo, in *Proceedings of the International Symposium on Microelectronics*, pp. 322-327 (1986).
8. C. L. Lau and G. K. Wertheim, *J. Vac. Sci. Technol.*, **15**, 622 (1978).
9. R. A. Powell, *App. Surf. Sci.*, **2**, 397 (1979).
10. S. C. Britton and K. Bright, *Metallurgia*, 163 (1957).
11. S. C. Britton and J. C. Sherlock, *Br. Corros. J.*, **9**, 96 (1974).
12. W. E. Boggs, P. S. Trozzo, and G. E. Pellissier, *J. Electrochem. Soc.*, **108**, 13 (1961).
13. R. Kurz and E. Kleiner, *Z. Werkstofftech.* 2, **8**, 418 (1971).
14. E. E. Kluizenaar, *J. Vac. Sci. Technol.*, **1**, 1480 (1983).
15. R. G. Miller and C. Q. Bowles, *Oxid. Met.*, **33**, 95 (1990).
16. E. Ricci, A. Passerone, and P. Castello, *J. Mater. Sci.*, **29**, 1833 (1994).
17. A. Passerone, E. Ricci, and R. Sangiorgi, *J. Mater. Sci.*, **25**, 4266 (1990).
18. R. Sangiorgi, C. Senillou, and J. C. Joud, *Surf. Sci.*, **202**, 509 (1988).
19. R. D. Deshmukh, M. F. Brady, R. A. Roll, and L. A. King, *Int. J. Microcircuits Electron. Packag.*, **16**, 97 (1993).
20. J. H. Lau, *Solder Joint Reliability, Theory, and Applications*, VanNostrand, Reinhold, New York (1991).
21. J. I. Ivankowits and S. W. Jacobs, *SMTCON Technical Proceedings*, pp. 283-300, Atlantic City, NJ (1990).
22. W. A. Oates and D. D. Todd, *J. Aust. Inst. Met.*, **7**, 109 (1962).
23. A. J. Bevolo, J. D. Verhoeven, and M. Noack, *Surf. Sci.*, **134**, 499 (1983).
24. O. Knacke, O. Kubatschewski, and K. Hesselmann, *Thermochemical Properties of Inorganic Substances*, Springer Verlag, Heidelberg (1991).

Downloaded 28 Jun 2010 to 192.38.67.112. Redistribution subject to ECS license or copyright; see http://www.ecsdl.org/terms_use.jsp